

Refractory glass–ceramics based on alkaline earth aluminosilicates

G.H. Beall

Corning Incorporated, Sullivan Park, One Science Center Drive, Corning, NY 14831, United States

Available online 8 October 2008

Abstract

Glass–ceramics that can be used at temperatures of 1200–1500 °C are found in the alkaline earth aluminosilicate field, and are generally nucleated internally with titania. These glass–ceramics have good strength (>100 MPa, abraded), can be tailored to produce high fracture toughness (2–5 MPa m^{1/2}), and have good dielectric properties. Coefficients of thermal expansion (CTEs) are low to moderate ((25–45) × 10⁻⁷ °C⁻¹, from 25 to 1000 °C).

The major crystalline phase in the glass–ceramics exhibiting the lowest CTEs is hexagonal cordierite (indialite), while important toughening accessory phases are enstatite and acicular magnesium dititanate.

The most refractory glass–ceramics that are easily melted at 1650 °C, yet when crystallized do not deform at 1450 °C, are based on strontium and barium monoclinic feldspars of the celsian type. CTEs range from 35 to 45 × 10⁻⁷ °C⁻¹. Acicular mullite is an important accessory phase aiding fracture toughness in these materials.

Mullite glass–ceramics which contain considerable siliceous residual glass are probably the most refractory of these glass–ceramics, but they require melting above 1700 °C. Nevertheless, they can be used at temperatures near 1600 °C.

Potential applications for refractory glass–ceramics include improved radomes, engine components, substrates for semiconductors and precision metallurgical molds.

© 2008 Elsevier Ltd. All rights reserved.

Keywords: Glass–ceramics; Nucleation; Refractory; Alkaline earths; Cordierite; Indialite; Enstatite; Sr-feldspar; Celsian; Mullite; Fracture toughness; Strength; Thermal expansion; Hardness; Modulus; Semiconductor substrates; Engine components; Metallurgical molds

1. Introduction

There are many advantages to glass–ceramics that are derived from internal nucleation and crystallization of bulk glass articles. Rapid commercial glass forming processes like rolling, pressing and casting may be used. A simple reheating process suffices to achieve a fine-grained and uniform microstructure with little or no porosity. The shape of the original glass article is preserved even as a high degree of crystallinity develops.

Glass–ceramics may be considered as refractory if they can be used at temperatures above 1200 °C. The most interesting of these are based on alkaline earth aluminosilicate compositions in the RO–Al₂O₃–SiO₂–TiO₂ system, where R is primarily Mg, Sr or Ba, and TiO₂ is the nucleating agent. In these glass–ceramics a combination of good flexural strength, hardness, fracture toughness, and resistance to both high temperature and thermal shock can be produced.

2. Experimental procedures

Glass batches, generally of 1 kg, were formulated from standard oxide materials, except in the case of CaO, SrO and BaO, where carbonates were used. Batches were mixed and melted between 1600 and 1650 °C in platinum crucibles and held for 16 h, except in the case of glasses designed to produce the most refractory mullite glass–ceramics, which were melted at 1800 °C in Pt–Rh crucibles for 4 h. All glasses were cast into 4 in. × 8 in. patties and annealed between 700 and 850 °C. The patties were heat-treated and converted to glass–ceramics. Bars of appropriate size were cut from the patties for physical property measurements.

For flexural strength (modulus of rupture) determinations, the samples were abraded and an MTS/Surtech tabletop testing machine was used according to ASTM Standards C-158-95B and C-158-02B. For fracture toughness measurements, the short bar technique was used.

For elastic moduli, the sonic resonance technique was used according to ASTM C623. Thermal conductivity was measured by the Precision Measurements and Instruments Corporation

E-mail address: BeallGH@corning.com.

(PMIC) using a Mathis TCi instrument. This test method uses a platinum hot disk sensor. A glass–ceramic specimen is placed on top of the sensor and a 500-g weight is placed on top of the sample to provide uniform contact.

Beam-bending viscosity was measured using ASTM C598 with a glass–ceramic beam of dimensions 0.1 in. \times 0.1 in. \times 3 in. Knoop hardness was measured according to ASTM C730.

Scanning electron microscopy was used to study microstructure of indialite and feldspar glass–ceramics. Both secondary electron and back-scatter techniques were helpful. In addition, platinum pre-shadowed replica electron microscopy was used for the mullite glass–ceramics.

3. Indialite (high cordierite) glass–ceramics in the MgO–Al₂O₃–SiO₂–TiO₂ System

3.1. Crystal chemistry

Indialite is the hexagonal modification and high temperature polymorph of cordierite and has identical stoichiometry: Mg₂Al₄Si₅O₁₈.¹ It differs from cordierite only in its random distribution of Al in the (Al,Si)₆O₁₈ ring, which raises the symmetry to the hexagonal point group 6/m 2/m 2/m and space group P6/mcc from that of orthorhombic cordierite of point group 2/m 2/m 2/m and space group Cccm. In addition, there is some solid solution permitted in the indialite composition from the Mg₂Al₄Si₅O₁₈ cordierite stoichiometry towards the hypothetical compound Mg–beryl (Mg₃Al₂Si₆O₁₈), but this is believed limited under equilibrium conditions to temperatures above 1300 °C.²

Indialite and cordierite have similar and low coefficients of thermal expansion (CTEs), about $16 \times 10^{-7} \text{ }^\circ\text{C}^{-1}$, measured from 25 to 1000 °C. They are both hard crystals, about 7.5 on the Mohs scale.³ Stoichiometric indialite melts incongruently to mullite and liquid at about 1470 °C.

3.2. Composition and properties

Glass–ceramics where indialite (high cordierite) is the predominant phase can be formed from glasses in a wide area in the central portion of the MgO–Al₂O₃–SiO₂ system. This area includes SiO₂ from 45 to 60 wt.%, Al₂O₃ from 17 to 40 wt.%, and MgO from 10 to 27 wt.%. Titania is added in amounts of 8–18 wt.% as an effective nucleation agent. Because of these TiO₂ additions, the glasses are amber in color. Although clear to the eye, slight scattering can be observed by a strong light beam, indicating the presence of a very fine phase separation.

Secondary crystal phases in these glass–ceramics may include enstatite (MgSiO₃), mullite (Al₆Si₂O₁₃), cristobalite (SiO₂), forsterite (Mg₂SiO₄), spinel (MgAl₂O₄), karronite (MgTi₂O₅), and rutile (TiO₂). All of these phases have much higher CTEs than indialite, so from a thermal shock point of view, the optimum glass–ceramic composition would be expected to approach that of stoichiometric cordierite with just enough titania added to allow good internal nucleation. Such a composition (No. 1 in Table 1) does give a low CTE of $23 \times 10^{-7} \text{ }^\circ\text{C}^{-1}$, only 7 points higher than that of indi-

alite itself, the difference being largely due to the contribution of accessory rutile formed from the titania added to insure good internal nucleation. There are practical problems with near-stoichiometric compositions, however. The combination of high liquidus temperature (>1450 °C) and low viscosity at the liquidus temperature allows rapid devitrification that creates difficulties in forming the glass and limits the thickness of a glass article.

In order to increase the stability of indialite-forming glasses, deviations in glass composition from stoichiometry are required. Deviations towards silica have the greatest effect in increasing glass viscosity while lowering liquidus temperature. Deviations towards enstatite also serve to lower the liquidus. In fact, the composition of the earliest “cordierite” glass–ceramic, Corning Code 9606 (No. 2, Table 1), was chosen to be near the eutectic cordierite–enstatite–silica² with titania additions for nucleation, in order to insure ease of centrifugal casting of missile nose cones (radomes). This glass–ceramic contains the crystalline assemblage indialite–cristobalite with minor enstatite, rutile and karronite. The cristobalite has the undesirable effect of raising the average CTE of the glass–ceramic to $45 \times 10^{-7} \text{ }^\circ\text{C}^{-1}$ from 25 to 1000 °C and even higher below 200 °C where the inversion of cristobalite from cubic to tetragonal occurs. One key advantage of the cristobalite is that it allows a caustic leaching process referred to as “fortification”⁴ to create a porous surface on radomes that protects the glass–ceramic from handling flaws, thus increasing its effective flexural strength after abrasion from about 150 MPa to over 350 MPa.⁵ The silica phase cristobalite is easily leached in caustic NaOH solution, whereas the other phases are resistant. Despite this high strength, it was felt that the hardness and fracture toughness, both important in missile use, could be improved with composition changes.

High values of fracture toughness ranging from 3.4 to 4.6 MPa m^{0.5} have been reported in glass–ceramic materials containing enstatite as the major phase.⁶ This toughness is believed largely due to energy absorption associated with twin and cleavage planes which tend to deflect, branch and blunt fractures. The observed lamellar twinning and resulting cleavage result from the martensitic transformation of protoenstatite to clinoenstatite, which occurs spontaneously on cooling. It was therefore deemed important to further explore indialite glass–ceramic compositions containing increased amounts of enstatite.

In order to develop more enstatite in indialite glass–ceramics, increasing the level of MgO relative to Al₂O₃ was required. In addition to decreasing the liquidus, thus improving glass stability, an unexpected benefit was discovered. The titania required for nucleation combined with the higher amounts of magnesia present tended to produce large amounts of the phase karronite: MgTi₂O₅. This titanate was observed to develop an acicular morphology in these indialite–enstatite glass–ceramics. This was expected to further increase fracture surface energy because of the reinforcement effect of this high modulus phase. In fact, fracture toughness values on some of these glass–ceramics were measured in the range of 2.5–4.4 MPa m^{0.5}, some values almost as high as those of the predominately enstatite glass–ceramics.

Table 1 lists a variety of indialite glass–ceramic compositions with the corresponding heat treatments, CTEs, E-moduli,

Table 1
Composition and properties of indialite (high cordierite) glass–ceramics in the SiO₂–Al₂O₃–MgO–TiO₂ system

wt. %	No. 1	No. 2 (9606)	No. 3	No. 4
SiO ₂	47.1	56.2	43.8	46.2
Al ₂ O ₃	28.5	19.8	24.7	15.6
MgO	13.3	14.7	18.7	22.1
CaO	0.0	0.1	1.4	1.5
TiO ₂	10.7	8.9	11.4	14.6
As ₂ O ₅	0.4	0.3	0.0	0.0
Major phases	Indialite Rutile	Indialite Cristobalite Rutile	Indialite Enstatite Karooite	Indialite Enstatite Karooite
Heat treatment	820 °C for 2 h 1260 °C for 8 h	820 °C for 2 h 1260 °C for 8 h	825 °C for 2 h 1200 °C for 10 h	825 °C for 2 h 1200 °C for 10 h
CTE ((25–1000) × 10 ⁷ °C)	23	44	41	54
E-modulus (GPa)	150	119	130	–
MOR (MPa)	130	155 ± 4	165 ± 6	164 ± 6
K _{1c} (MPa m ^{0.5})	–	2.2 ± 0.2	4.3 ± 0.4	3.4 ± 0.7
KHn	–	700	984 ± 16	842 ± 16
Thermal conductivity (W/mK at 25 °C)	–	3.75	4.01	–

flexural strengths (abraded) and values of hardness, fracture toughness and thermal conductivity. The thermal stability of these materials is limited to 1250 °C, but mechanical properties are of special interest. Glass–ceramic No. 3 showed a combination of high hardness, toughness and E-modulus, with good strength. Fig. 1 illustrates the microstructure of this glass–ceramic. Note the acicular morphology of the karrooite phase.

It is interesting that the density of the glass–ceramic No. 3 (2.779 ± 0.001 g/cm³) is actually less than that of the parent glass (2.787 ± 0.001 g/cm³), indicating a small net volume expansion of about 0.3%. This is perhaps not surprising, as indialite is an open framework structure with a low measured density of 2.51 g/cm³.³

Small additions of CaO to these indialite glass–ceramics were useful. Cracking during the crystallization process can occur with thick pieces where stresses due to large density changes during the metastable crystallization sequence (see Section 3.3) are amplified by thermal gradients in the sample. Calcium oxide

additions of from 0.5 to 2% serve to reduce or eliminate such cracking. An accessory phase: anorthite: CaAl₂Si₂O₈ may form as a result of these additions.

3.3. Phase development during heat treatment

The development of crystalline phases in Code 9606 (No. 2, Table 1) has recently been described.⁷ The sequence of crystallization of a typical indialite–enstatite–karrooite glass–ceramic (No. 3, Table 1) is somewhat different, and was determined by heating the parent glass to the nucleation temperature of 825 °C for 2 h and then to various increasing higher temperatures for 4 h. The first crystalline phase to precipitate at temperatures near 825 °C is a magnesium aluminum titanate solid solution along the join karrooite (MgTi₂O₅)–tielite (Al₂TiO₅).⁸ On further heating to 850 °C, the first silicate phase, metastable petalite forms.⁹ This phase is replaced as crystallization proceeds at 900 °C by other metastable phases: β-quartz solid solution and aluminous enstatite. The former is a stuffed derivative of β-quartz, sometimes referred to as μ-cordierite, where Al³⁺ replaces Si⁴⁺ in the quartz network and the charge is made up by Mg²⁺ ions stuffing the cavities in the double helix of β-quartz.^{10,11} Aluminous enstatite contains considerable substitution of aluminum into the structure according to 2Al³⁺ for Mg²⁺ + Si⁴⁺ along the join enstatite–pyrope (MgSiO₃–Mg₃Al₂Si₃O₁₂).^{12,13} Spinel begins to exsolve from the β-quartz solid solution at 950 and 1000 °C, the quartz becomes very siliceous and is essentially α-quartz. At this point the maximum density, 3.06 g/cm³ is reached, indicating a volume-shrinkage at this stage of about 10%. A small amount of indialite also appears at 1000 °C as aluminous enstatite begins to fade. By 1050 °C, volume expansion occurs as the low-density indialite (2.51 g/cm³) becomes the predominant phase, quartz disappears and aluminous enstatite and karrooite both lose their alumina. Some spinel remains, and rutile makes an appearance. At 1100 °C, the phase assemblage is essentially

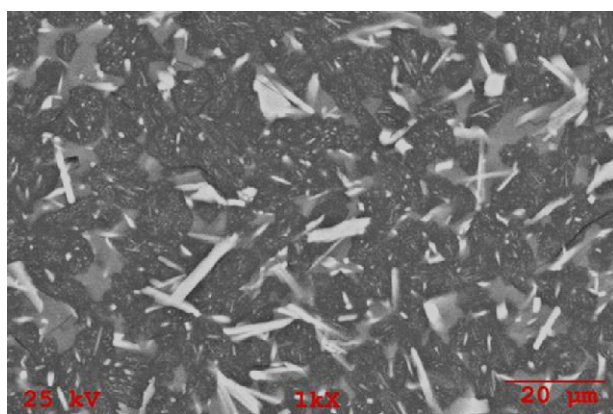


Fig. 1. Back-scattered scanning electron micrograph (SEM) of tough indialite (dark matrix) glass–ceramic No. 3 with enstatite (grey) and acicular karrooite (white).

Table 2
Composition and properties of feldspar and mullite glass–ceramics in the $\text{SiO}_2\text{--Al}_2\text{O}_3\text{--SrO--BaO--TiO}_2$ system

wt. %	No. 5	No. 6	No. 7	No. 8	No. 9
SiO_2	34.1	36.9	35.8	35.5	45.0
Al_2O_3	32.9	33.2	30.3	32.1	40.0
SrO	23.9	21.6	0.0	14.5	0.0
BaO	0.0	0.0	25.7	9.6	10.0
TiO_2	9.1	8.3	8.2	8.3	0.0
Heat treatment	850 °C for 2 h 1425 °C for 6 h	850 °C for 2 h 1425 °C for 6 h	850 °C for 2 h 1425 °C for 6 h	850 °C for 2 h 1425 °C for 6 h	1500 °C for 6 h
Crystal phases	Sr-feldspar Tielite	Sr-feldspar Tielite Mullite	Celsian Mullite Tielite	Celsian Tielite Rutile	Mullite
CTE ($(25\text{--}1000) \times 10^{-7} \text{ }^\circ\text{C}$)	43	37	41	–	36
MOR (MPa)	132 ± 17	–	105 ± 10	–	–
K_{1c} (MPa m ^{0.5})	2.67 ± 0.20	2.22 ± 0.05	1.72 ± 0.04	–	–

indialite–enstatite–karrooite, and this remains constant until 1200 °C, where a small amount of anorthite can be observed as an accessory phase.

4. Strontium-feldspar and celsian glass–ceramics in the $\text{SrO--BaO--Al}_2\text{O}_3\text{--SiO}_2\text{--TiO}_2$ system

4.1. Crystal chemistry

Strontium-feldspar: $\text{SrAl}_2\text{Si}_2\text{O}_8$, is a monoclinic framework structure of point group $2/m$ and space group $I2/c$.¹⁴ It is closely related in structure with identical space group to the Ba-feldspar:celsian ($\text{BaAl}_2\text{Si}_2\text{O}_8$), and has sometimes been referred to as Sr-celsian. Strontium-feldspar is stable under ambient pressure at all temperatures up to its congruent melting temperature slightly below 1700 °C.¹⁵

Celsian is a naturally occurring feldspar of barium: $\text{BaAl}_2\text{Si}_2\text{O}_8$. There is wide if not complete miscibility between celsian and Sr-feldspar, and a minimum melting point of these solid solutions occurs at 1675 °C and 25 mol% celsian.¹⁵ Celsian itself converts to a high-temperature hexagonal polymorph known as hexacelsian above 1590 °C.¹⁶ Hexacelsian melts congruently near 1740 °C.¹⁵ This hexagonal structure is a layered silicate, and is not considered a feldspar,¹⁷ although it has identical stoichiometry to celsian. Hexacelsian has a high thermal expansion with an upward displacement in the range 270–400 °C,¹⁸ and its presence in glass–ceramics is therefore undesirable. A similar hexagonal polymorph of $\text{SrAl}_2\text{Si}_2\text{O}_8$ exists as a metastable form, and has a similar hook in its expansion curve, in this case near 600 °C.¹⁹

4.2. Composition and properties

Internally nucleated glass–ceramics have been previously described from glasses of compositions around alkaline earth feldspar compositions.²⁰ Small amounts (≤ 1 wt.%) of MoO_3 , V_2O_5 and the noble metals rhodium and iridium were added as nucleating agents. No actual strontium or barium feldspars were reported, however. Only the hexagonal polymorphs hexacelsian

and its strontium and calcium analogs were present. Unfortunately, these glass–ceramics all possess high thermal expansion behavior (CTEs $\geq 65 \times 10^{-7} \text{ }^\circ\text{C}^{-1}$, 25–1000 °C) exacerbated by the phase inversion associated with these layered structures. In addition, the parent glasses required melting at 1800 °C.

We have found that glass–ceramics with monoclinic Sr-feldspar as the major phase can be made from a significant area of ternary glasses in the $\text{SrO--Al}_2\text{O}_3\text{--SiO}_2$ system, with necessary additions of about 8–15 wt.% of TiO_2 to insure effective internal nucleation. This area is illustrated in Fig. 2, superimposed on the liquidus phase diagram,²¹ which is given in mol%. With the additions of titania, these glasses are easily melted at 1650 °C. It is interesting to note that this area of good glass formation, even with the TiO_2 additions, stretches below 50 mol% of SiO_2 , suggesting that SrO, unlike BaO and MgO, but more like CaO, increases the glass-forming ability of Al_2O_3 .

The most outstanding property of Sr-feldspar glass–ceramics is their refractory character; they can be held for many hours at 1450 °C without noticeable deformation. The crystalline assemblage is normally Sr-feldspar–tielite (Al_2TiO_5) but mullite and

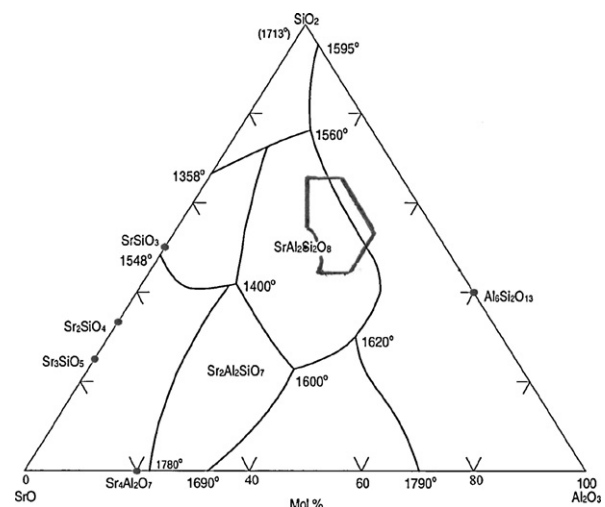


Fig. 2. Area of refractory titania-nucleated Sr-feldspar glass–ceramics in the $\text{SiO}_2\text{--Al}_2\text{O}_3\text{--SrO}$ system (mol%).

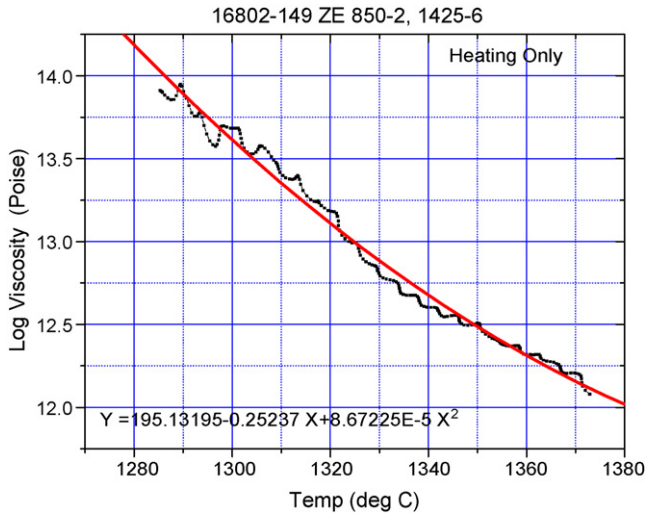


Fig. 3. Beam-bending viscosity vs. temperature for Sr-feldspar glass–ceramic No. 5; apparent annealing point = 1325 °C.

free TiO_2 in the form of rutile or anatase may also be present. Typical compositions are listed in Table 2, with heat treatment and property data. Glass–ceramic No. 5 is very highly crystalline and composed almost entirely of Sr-feldspar and tielite. Deformation was studied by placing a 5 in.-bar of 0.21 in. thickness across a 4 in.-span and holding for 6 h at 1425 °C. Less than 0.04 in. sag was observed. A bending-beam viscosity measurement revealed an apparent annealing point ($\eta = 10^{12}$ Pa s) of 1325 °C (Fig. 3). This glass–ceramic represents the most refractory bulk-glass-derived material to date that can be melted at the commercially feasible temperature of 1650 °C. Volume shrinkage during crystallization is about 1.7%, the parent glass having a density of 2.99 g/cm³ and the glass–ceramic 3.04 g/cm³.

Other properties of note for this composition include fracture toughness (K_{Ic}) of 2.7 MPa m^{0.5} and flexural strength after abrasion of 130 MPa, despite the presence of microcracks and occasional pores, as seen in Fig. 4. Since the parent glass had no porosity, it is assumed that these pores developed through cavitation as the glass crystallized. This could be associated with rapid crystallization and insufficient residual glass to allow shrinkage

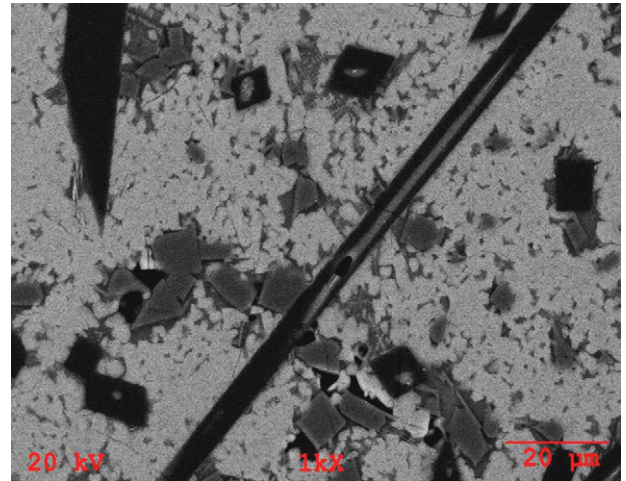


Fig. 5. Back-scattered SEM showing microstructure of multiphase Sr-feldspar–mullite–tielite glass–ceramic No. 6 (note finer light feldspar laths and larger dark acicular mullite).

without void formation. The appearance of microcracks is also evidence of the absence of significant residual glass. There is well-known anisotropy of CTE in the tielite phase, which as a conventional ceramic is highly microcracked.²² There are also CTE differences in the lattice directions of feldspars and between Sr-feldspar and tielite. With little glassy phase present, differential stresses developing along grain boundaries during cooling cannot be easily relieved. Microcracks may also be responsible for the relatively high toughness of this glass–ceramic because they tend to deflect, blunt or cause branching in fracturing. The degree of microcracking, however, is not large enough to cause hysteresis in the thermal expansion curve, which is identical on both heating and cooling.

Sr-feldspar glass–ceramic compositions higher in Al_2O_3 form mullite as a secondary phase (e.g. No. 6, Table 2). This phase grows in large acicular habit (Fig. 5) and may be responsible for the moderately good toughness (2.2 MPa m^{0.5}) of this glass-containing, non-microcracked and non-porous composition.

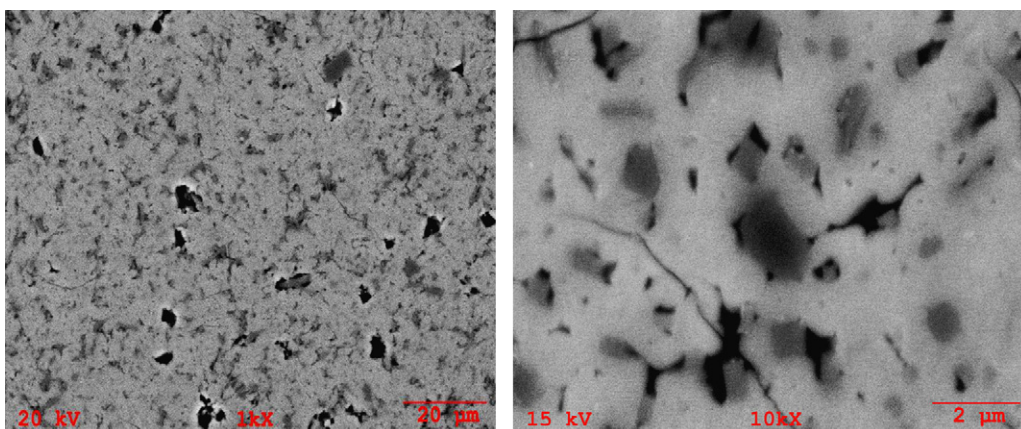


Fig. 4. Back-scattered SEM showing microstructure of Sr-feldspar glass–ceramic No. 5 at two different magnifications (note interlocking feldspar laths, microcracks and cavitation pores).

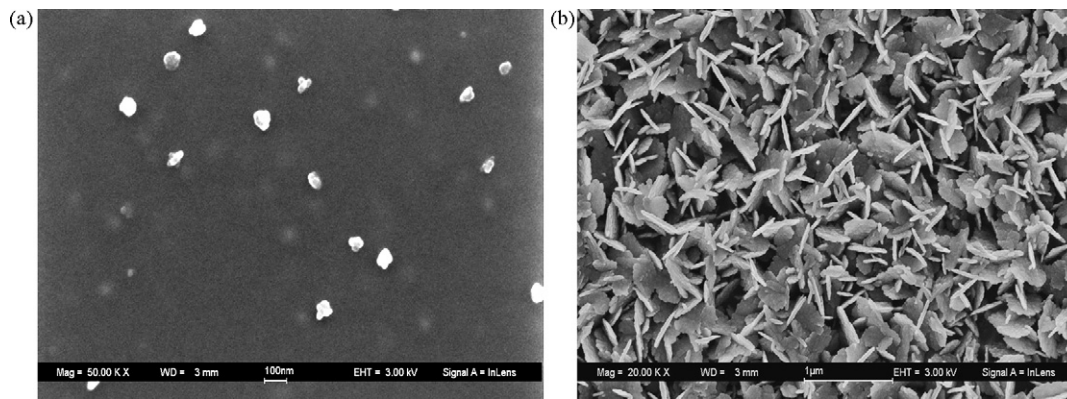


Fig. 6. Secondary electron image of κ -alumina-structured nuclei, probably Al_4TiO_8 , in glass No. 5 heated at 850 °C for 4 h (left) and at 875 °C for 4 h (right) with glass preferentially etched (note scale difference).

In contrast to the Sr-aluminosilicates, the refractory glass–ceramic-forming area in the BaO– Al_2O_3 – SiO_2 system with TiO_2 additions necessary for nucleation of celsian is very restrictive. It basically consists of a small region around the celsian–mullite–alumina eutectic on the ternary liquidus phase diagram²³ near 1580 °C at about 39 wt.% SiO_2 , 32 wt.% Al_2O_3 , and 29 wt.% BaO, with TiO_2 additions of 7.5–11 wt.%. Table 2 shows a typical celsian glass–ceramic composition (No. 6) and a mixed celsian–Sr-feldspar solid solution composition (No. 7). Heat treatment and property data are also shown. Volume shrinkage on crystallization for glass No. 6 is about 2.6%, the parent glass having a density of 3.08 g/cm³ and the glass–ceramic 3.16 g/cm³.

There does not seem to be any property advantage to the celsian glass–ceramics over their Sr-feldspar counterparts, unless higher density is required. The celsian materials may be somewhat finer grained, perhaps because of their considerable content of siliceous residual glass. In general there also seems to be slightly more deformation on crystallization. Solid solution glass–ceramics intermediate between celsian and Sr-feldspar also appear to have no advantages over the Sr-feldspar end-member materials.

One important general feature of Sr–Ba-feldspar glass–ceramics is the ability to tailor the CTE in the range of $(30\text{--}50) \times 10^{-7} \text{ }^\circ\text{C}^{-1}$. This is accomplished by varying

the amount of accessory phases, particularly CTE-lowering siliceous residual glass, in order to allow the glass–ceramic to match important ceramic materials like silicon, silicon carbide and silicon nitride.

In terms of solid solutions of various alkaline earth feldspars, it is interesting that Ca-feldspar, anorthite ($\text{CaAl}_2\text{Si}_2\text{O}_8$), which is triclinic, does not produce good glass–ceramics, even with large amounts of added titania (~ 15 wt.% TiO_2). Large scale deformation and/or coarse crystallization from the surface result from heat treatment of such glasses. In feldspar mixtures or in solid solution, some anorthite component can be tolerated in Sr–Ba-feldspar glass–ceramics, but levels in excess of 4 wt.% CaO tend to reduce use temperatures below 1400 °C.

4.3. Phase development during heat treatment

The sequence of phases developing during heat treatment of Sr-aluminosilicate glass No. 5, Table 2 was determined by heating at the nucleation temperature of 875 °C for 4 h and then heating to various higher temperatures for 4 h. This glass, as is typical for all parent glasses of titania-nucleated feldspar glass–ceramics, is originally clear with an amber color. It shows slight scattering in a strong light beam.

The first indication of crystallization occurs near 850 °C where broad X-ray diffraction peaks reveal a pattern identical

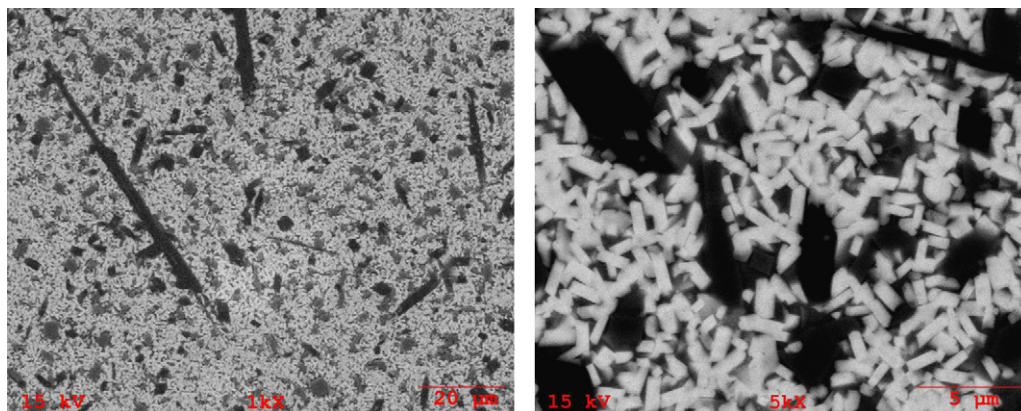


Fig. 7. Back-scattered SEM showing microstructure of celsian–mullite–tietite glass–ceramic No. 7 (note fine celsian laths and coarse acicular mullite).

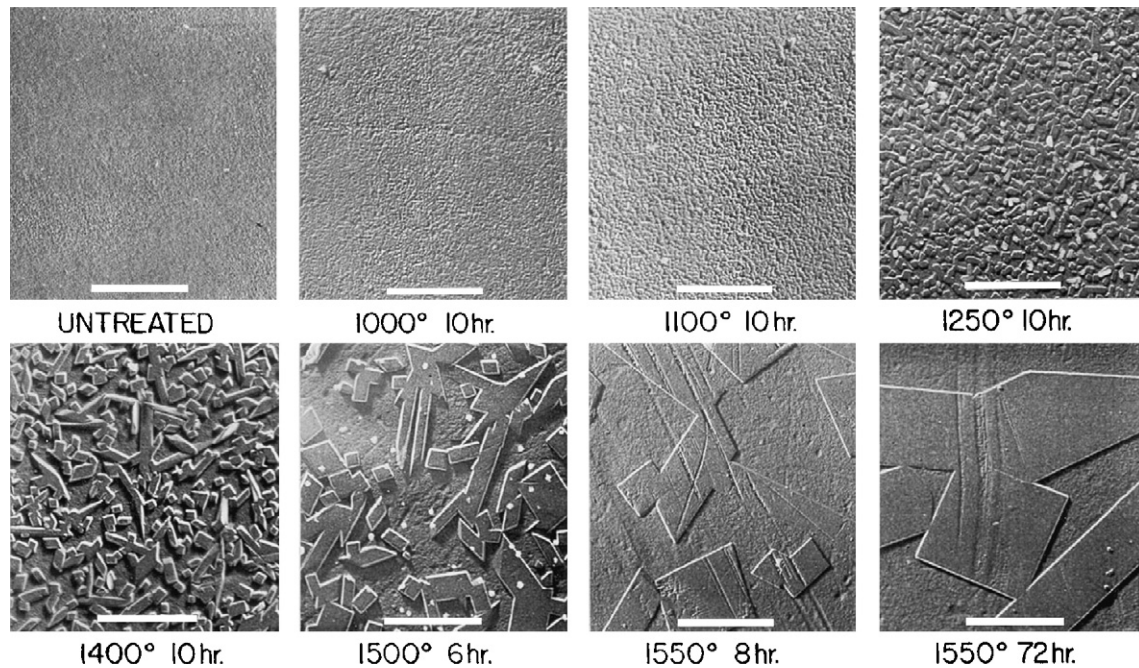


Fig. 8. Crystallization of a mullite glass–ceramic (replica electron microscopy after MacDowell).

to a rare form of alumina, κ - Al_2O_3 .²⁴ This phase was originally synthesized by heating the clay mineral tohdite, $\text{Al}_5\text{O}_7(\text{OH})$, and it retains the basic oxide lattice of the tohdite structure with some Al-cation vacancies.²⁴ In the case of our glass–ceramic, one would expect some titania to be substituted within the structure of these nanocrystals, because without substantial TiO_2 in the composition, the κ -alumina-type phase does not form and internal nucleation does not occur. It therefore seems probable that substitution of titanium for aluminum in tetrahedral sites of the tohdite structure has occurred as $\text{Ti}^{4+} + \text{O}^{2-} \rightarrow \text{Al}^{3+} + (\text{OH})^-$. According to this idea, the actual κ -alumina structure responsible for internal nucleation in this glass would then be expected to be Al_4TiO_8 , or $2\text{Al}_2\text{O}_3 \cdot \text{TiO}_2$. These small (<100 nm) nuclei can be seen as scattered platy particles at 850 °C and they grow in number and size (~500 nm) at 875 °C. They are readily observed by back-scatter electron microscopy on fracture surfaces where the glass has been preferentially etched (Fig. 6). A comparison of the etched and non-etched surfaces by energy dispersed X-ray spectroscopy (EDX) does indicate that these crystallites are enriched in alumina and titania relative to the surrounding glass.

The first silicate phase to crystallize near 950 °C is the metastable hexagonal form of $\text{SrAl}_2\text{Si}_2\text{O}_8$, accompanied by free titania in the form of rutile (TiO_2), as the κ -alumina phase begins to disappear. This hexagonal layered silicate has a high CTE with a hook in its expansion curve near 600 °C¹⁵ and is therefore undesirable from the standpoint of thermal shock resistance. This metastable phase persists until between 1100 and 1150 °C, where it transforms completely to the stable monoclinic Sr-feldspar. All traces of the κ -alumina-type nuclei are gone by this stage. Above 1200 °C, tielite forms and rutile begins to disappear. By 1425 °C, only a trace of rutile can be found.

The sequence of phases and transformations occurring during heat treatment of Ba-aluminosilicate glass No. 7 is simpler.

As in the case of the Sr-feldspar glass–ceramics, a structure resembling κ -alumina, probably Al_4TiO_8 , is the first crystal to form near 875 °C. At 925 °C, celsian can be observed by X-ray diffraction and microscopy to form, along with a replacement of the κ -alumina by Al_2TiO_5 (tielite). It is suspected that the celsian is nucleated directly by the κ -alumina-type phase rather than by the later-forming tielite. Mullite appears to be the last phase to crystallize above 1100 °C. The final assemblage after heat treatment to 1425 °C consists of four phases: celsian, tielite, mullite and siliceous glass. These can be distinguished by EDX performed on the fracture surfaces seen in the micrographs of Fig. 7. Note the large acicular form of mullite (black) contrasting with the smaller prismatic celsian crystals and the grey tielite. The siliceous glass appears as black irregular areas.

It is notable that metastable hexacelsian does not form at any temperature in this composition, although it is readily observed as a metastable phase in similar compositions containing less titania.

5. Mullite glass–ceramics

5.1. Crystal chemistry

Mullite ($3\text{Al}_2\text{O}_3 \cdot 2\text{SiO}_2$) is a defect-derivative structure of sillimanite ($\text{Al}_2\text{O}_3 \cdot \text{SiO}_2$) in which 2Al^{3+} cations replace 2Si^{4+} cations and one O^{2-} anion is removed from the structure producing a tri-bridged oxide ion.²⁵ The general structure can be given as $\text{Al}_{4+2x}\text{Si}_{2-2x}\text{O}_{10-x}$, where x has been observed to vary from 0.17 to 0.59, but is typically very near 0.25 as in the case of stoichiometric mullite. Mullite is orthorhombic with point group symmetry of $2/m\ 2/m\ 2/m$ and space group $Pbam$. It has an average CTE of $48 \times 10^{-7} \text{ }^\circ\text{C}^{-1}$ from 20 to 1000 °C,²⁶ and often displays acicular morphology.

5.2. Composition, phase development and properties

Mullite glass–ceramics with extraordinary refractoriness have been produced from binary Al_2O_3 – SiO_2 glasses with minor additions of BaO .²⁶ The glasses require a melting temperature above 1750°C , and show internal nucleation without the aid of a nucleating agent. Fig. 8 shows a series of replica electron micrographs illustrating the growth of mullite from a ternary aluminosilicate glass containing 30 mol% alumina and 5 mol% BaO (No. 8, Table 2). Mullite can be observed by X-ray diffraction at 950°C and can be seen here as a fine texture at 1000°C . These nanocrystals grow with increasing temperature and become euhedral above 1200°C . By 1400°C the crystals grow to $1\ \mu\text{m}$ in length, and after heat treatment at 1550°C for 72 h, they reach $1\ \mu\text{m}$ in width and several micrometers in length. The nucleation has been described as a result of phase separation in the binary alumina–silica system,²⁶ and the addition of baria deemed essential to prevent crystallization of the high-CTE cristobalite phase²⁶.

The key properties of these mullite glass–ceramics are their high use temperature, at least to 1550°C for long periods, without showing noticeable deformation. The CTEs are also relatively low, at about $36 \times 10^{-7}^\circ\text{C}^{-1}$, and the densities near $2.8\ \text{g/cm}^3$. Flexural strengths are about 100 MPa.

6. Potential applications

6.1. Indialite glass–ceramics

Corning Code 9606 glass–ceramic, based largely on indialite and cristobalite, has been used for 50 years as a missile nose cone material. Its advantages include good strength and thermal shock resistance, a thermal use temperature of 1250°C , and good dielectric properties allowing transparency to microwave energy used to guide the missile. One area where improvement is desired is in resistance to rain erosion. Modern missiles are fired with increasing speed through rain and clouds. This requires higher hardness and fracture toughness. Major improvements in both these properties have been achieved in new compositions with the crystal assemblage indialite–enstatite–karrooite (Table 1).

Besides radomes, other applications for the new harder and tougher indialite glass–ceramics are envisioned. It is expected that these materials would have some advantages over other hard and tough high temperature ceramics like silicon nitride, silicon carbide and alumina. These include lower density, better thermal shock resistance, oxidation resistance, zero porosity and a very uniform microstructure with a resulting low defect level. Engine components are a possible area of application.

6.2. Sr-feldspar and celsian glass–ceramics

As with indialite glass–ceramics, there could be high temperature engine component application for Sr-feldspar–celsian glass–ceramics. These materials would have the advantage in thermal stability with use temperatures above 1400°C , but fracture toughness, hardness, and density would be somewhat inferior.

The application of Sr–Ba feldspar glass–ceramics as suitable substrates for semiconductors, particularly silicon, is of particular interest. These glass–ceramics can be made to match silicon ($\sim 35 \times 10^{-10}^\circ\text{C}^{-1}$) in CTE, and with use temperatures up to and above the melting point of silicon, the substrates could be coated with molten silicon that could be subsequently crystallized just below its melting point of about 1415°C . At such high temperatures, grain growth kinetics would be rapid and nucleation sites limited. Large-grain silicon films would result, with photovoltaic advantages over finer grained silicon.

Because of the ability to match CTEs with those of silicon carbide and silicon nitride, these feldspar–glass–ceramics could be useful as joining materials for these high temperature ceramics.

Refractory Sr–Ba feldspar glass–ceramics might also be considered as suitable material for precision molds for molten metal casting, perhaps at temperatures at or even exceeding 1450°C , necessary for some superalloys. The fine-grained and non-porous nature of the glass–ceramics would allow high surface quality, and the mold shape could be closely simulated in casting the original glass.

6.3. Mullite glass–ceramics

For use at more extreme temperatures above 1500°C , mullite glass–ceramics can be considered, despite the limitation of a required melting temperature for these materials of 1800°C . Again, such materials could be considered for superalloy casting, engine components and substrates for silicon and other semiconductors.

Acknowledgements

The author would like to thank Dr. Linda R. Pinckney for her helpful discussions and support of this research. He also thanks John Bartoo for his electron microscope work and Mr. Steve Tietje for his technical support.

References

- Hurlbut, C. S. and Klein, C., (19th ed.). *Manual of Mineralogy* John Wiley and Sons, 1977, p. 368.
- Schreyer, W. and Schairer, J. F., Compositions and structural states of anhydrous Mg–cordierites: a re-investigation of the central part of the system MgO – Al_2O_3 – SiO_2 . *J. Petrol.*, 1961, **2**, 324–406 [Part 3].
- Anthony, J. W., Bideaux, R. A., Bladh, K. W. and Nichols, M. C., *Handbook of Mineralogy*, vol. 161. Mineral Data Publishing, 1995, p. 367.
- Beall, G. H. and Doman, R. C., Glass–ceramics. *Encyclop. Phys. Sci.*, 1987, **6**, 302.
- Lewis III, D. L., Observations on the strength of a commercial glass–ceramic. *Bull. Am. Ceram. Soc.*, 1982, **61**(11).
- Echeverria, L. M. and Beall, G. H., Enstatite ceramics: glass and gel routes, ceramic transactions. *Am. Ceram. Soc.*, 1991, **20**, 235–244.
- Lee, W. E., Arshad, S. E. and James, P. F., Importance of crystallization hierarchies in microstructural evolution of silicate glass–ceramics. *J. Am. Ceram. Soc.*, 2007, **90**(3), 727–737.
- Phase Equilibria Diagrams: No. 714, CD-ROM Database, NIST*. Am. Ceram. Soc., 2005.
- Schreyer, W. and Schairer, J. F., Metastable osumilite and petalite solid solutions in the system MgO – Al_2O_3 – SiO_2 . *Am. Miner.*, 1962, **47**, 90–104.

10. Schreyer, W. and Schairer, J. F., Metastable solid solutions of with quartz-type structures on the join $\text{SiO}_2\text{--MgAl}_2\text{O}_4$. *Z. Krist.*, 1961, **116**, 60–82.
11. Beall, G. H., Karstetter, B. R. and Rittler, H. L., Chemical strengthening of stuffed β -quartz glass–ceramics. *J. Am. Ceram. Soc.*, 1967, **50**, 99–108, no. 4.
12. Deubener, J., Nucleation kinetics of aluminous enstatite in pyrope glass ($3\text{MgO}\cdot\text{Al}_2\text{O}_3\cdot 3\text{SiO}_2$). *Phys. Chem. Glass*, 2004, **43**, 259–262 [Part C; SPI].
13. Rubin, A. E., Aluminian low-Ca pyroxene in a Ca–Al-rich chondrule from the Semarkona Meteorite. *Am. Miner.*, 2004, **89**, 867–883.
14. Chiari, G., Calleri, M. and Bruno, E., The structure of partially disordered, synthetic strontium feldspar. *Am. Miner.*, 1975, **60**, 111–119.
15. *Phase Equilibria Diagrams: No. 10784, CD-ROM Database, NIST*. Am. Ceram. Soc., 2005.
16. Bahat, D., Kinetic study of the hexacelsian–celsian phase transformation. *J. Mater. Sci.*, 1970, **5**, 805–810.
17. Ribbe, P. H., Chemistry, structure and nomenclature of feldspars (2nd ed.). *Feldspar Mineralogy, vol. 2* Mineralogical Soc. Am, 1983, pp. 2–3.
18. Bahat, D., Homogeneous and heterogeneous polymorphic transformations in alkaline earth feldspars. *J. Mater. Sci.*, 1978, **13**, 2548–2554.
19. Bahat, D., Several metastable alkaline earth feldspar modifications. *J. Mater. Sci.*, 1972, **7**, 198–200.
20. Bahat, D., Compositional study and properties characterization of alkaline earth feldspar glasses and glass–ceramics. *J. Mater. Sci.*, 1969, **4**, 855–860.
21. *Phase Equilibria Diagrams: No. 10673, CD-ROM Database, NIST*. Am. Ceram. Soc., 2005.
22. Yutaka, O., Nakagawa, Z. and Hamano, K., Grain-boundary microcracking due to thermal expansion isotropy in aluminum titanate ceramics. *J. Am. Ceram. Soc.*, 1987, **70**(8), C184–C186.
23. *Phase Equilibria Diagrams: No. 556, CD-ROM Database, NIST*. Am. Ceram. Soc., 2005.
24. Okumiya, M. and Yamaguchi, G., The crystal structure of $\kappa\text{-Al}_2\text{O}_3$, the new intermediate phase. *Bull. Chem. Soc. Jpn.*, 1971, **44**, 1567–1570.
25. Angel, R. J. and Prewitt, C. T., Crystal structure of mullite: a re-examination of the average structure. *Am. Miner.*, 1986, **71**, 1476–1482.
26. MacDowell, J. F. and Beall, G. H., Immiscibility and Crystallization in $\text{Al}_2\text{O}_3\text{--SiO}_2$ glasses. *J. Am. Ceram. Soc.*, 1969, **52**(1), 37–45.